The International Journal of Advanced Manufacturing Technology (2019) 100:2669–2678
https://doi.org/10.1007/s00170-018-2845-5

ORIGINAL ARTICLE

Automated vision positioning system for dicing semiconductor chips using improved template matching method

Fengjun Chen [1,2] · Xiaoqi Ye [1] · Shaohui Yin [1,2] · Qingshan Ye [2] · Shuai Huang [1] · Qingchun Tang [1]

Received: 29 May 2018 / Accepted: 3 October 2018 / Published online: 19 October 2018

Abstract

This study proposes an automated vision positioning system to realize high-efficient and high-precision positioning and dicing of semiconductor chips in an automatic dicing saw. In this method, image pyramid construction was established to improve the searching speed of feature images by using the pyramid hierarchical search strategy. Hough transformation was used to obtain the approximate angle of the feature images of the semiconductor chips. The improved template matching approach based on the initial angle was proposed to rapidly calculate rotation angle and feature position. Polynomial fitting was adopted to achieve sub-pixel positioning accuracy. Experimental results showed that the proposed algorithm can realize high-precision and real-time recognition under the weak light, strong light, uneven illumination, and rotation angle. The success rate is 99.25%, and the time consumed is only 1/4 of the normalized cross-correlation algorithm. The vision positioning and dicing experiment of the semiconductor chips was carried out on a high-precision dicing saw. The results confirm that the improved algorithm could be used for high-precision and real-time dicing semiconductor chips.

Keywords Vision positioning · Template matching · Dicing · Semiconductor chips

1 Introduction

Semiconductor chips are widely used in optics and electronic information field. The dicing process of semiconductor chips consists of seven main procedures: loading, delivery, automatic alignment, dicing, kerf check, cleaning, and unloading. A precision dicing saw is responsible for high-precision and high-efficient dicing of semiconductor chips [1]. Vision positioning is a key technology used in full automatic dicing processes [2]. A matching algorithm including pixel intensity–based and feature-based algorithms [3] is important to achieve the effective vision positioning. The pixel intensity–based algorithm exhibits the advantages of simple computation and high precision. However, this algorithm cannot be easily applied when the target has large disturbances, such as being covered or fragmentary, when an angle occurs or when the size changes. By contrast, the feature-based algorithm can match the target by searching the line, corner points, and contour features. The algorithm exhibits good adaptability and strong robustness, but it is complex and consumes much time to extract and analyze geometric features.

An orthogonal matching pursuit algorithm could be used to reconstruct the surface defect image and remove the Gauss noise [4]. Peng and Xu [5] proposed a hash-based template matching method to improve the efficiency and precision based on the line-by-line search strategy. Bao et al. [6] reported a solution for the problems of multi-angle and dimension cucumber recognition by establishing a multi-template matching library with a certain proportional scaling and rotation steps; however, this library was limited due to increased computational load. Kim [7] used Hough transform to obtain a robust template matching for scaling, partial occlusions, and rotation. The normalized cross-correlation was used for local matching target and global optimization [8]. Mattoccia et al. [9] presented a fast template matching algorithm based on the zero-mean normalized cross-correlation to decrease the computational burden. Yu and Fei [10] suggested a good applicable algorithm based on pyramid model and high moments to match screw objects; however, this algorithm cannot be easily

✉ Fengjun Chen
abccfj@126.com

[1] National Engineering Research Center for High Efficiency Grinding, Hunan University, Changsha 410082, Hunan, China

[2] Changsha Huateng Intelligent Equipment Co. Ltd., Changsha 410061, Hunan, China

applied to incomplete contour objects. Liang et al. [11] combined image pyramid with the Hessian matrix and used the steepest descent method to remove false matches. Matsuda et al. [12] proposed an approach to authenticate finger-vein. Cui et al. [13] introduced the distance transform and fuzzy model to match the fiducial mark alignment. In order to solve image registration, Yan et al. [14] proposed an iterative multiplicative updating algorithm and unsupervised manifold alignment. A new shape matching method was proposed based on the skeleton with Chordal Axis Transform [15]. Yang et al. [16] developed an improved method by reusing the pruned skeleton branches and put forward the similarity computation method among hierarchical skeletons. Zhong et al. [17] proposed a blob analyzation-based template matching algorithm to locate LED chip. The chip positioning accuracy can be improved by improving the camera calibration algorithm of LED chip visual positioning system [18]. A matching method based on gradient orientations was insensitive to illumination [19] but could not adapt to multi-angle and dimension object. These above algorithms can be summarized into two categories. First, the geometric-features-based algorithms can improve the adaptability and accuracy but cannot satisfy the real-time requirements because of the longtime consumption. Second, the improved template matching algorithm enhances the search strategy and shortens time consumption but cannot improve the applicability.

An automated vision positioning system was reported for rapid high-accuracy positioning of dicing semiconductor chips in a dicing saw. In this method, image pyramid construction was established to improve the searching speed of feature images by using the pyramid hierarchical search strategy. The improved template matching approach based on initial angle was proposed to rapidly calculate rotation angles and feature positions. The positioning and dicing experiment of the semiconductor chips was carried out to verify the validity and accuracy of the improved algorithm.

2 Methods

2.1 Positioning progress

Accurately placing semiconductor chip workpiece and manually confirming the dicing position are difficult in a precision dicing saw. The on-machine vision positioning system (VPS) can automatically determine the dicing position through the image recognition technology. Fig. 1a shows the sketch of VPS in an automatic dicing saw. When eight rectangular workpieces with many semiconductor chips are placed on the workbench (Fig. 1b), the vision system begins to search for a pair of special marks by an image matching algorithm. The angle θ and the coordinates at the points p1 and p2 of the special marks are obtained (Fig. 1c). After converting the image coordinates into the machine coordinates, the correction angles and starting positions are calculated to dice the semiconductor chips. Obtaining the accurate positions and angles of these special marks in eight workpieces is extremely important. The position error should be less than 1 pixel, and the angle error should be less than 0.1°. The number of pixels in the template image is set within 50,000–80,000. The time consumption should be less than 80 ms, and the number of matching targets may be more than one.

2.2 Positioning method

2.2.1 Flow of position matching

To satisfy the vision positioning requirements for high-precision dice semiconductor chips, an improved template matching algorithm was proposed, as shown in Fig. 2; the flowchart is illustrated as follows:

Step 1: Creat the image pyramid construction of the template and pre-processed images.
Step 2: Apply Hough transformation to the highest-level image of the image pyramid and obtain an approximate angle value of the workpiece image.
Step 3: Perform a complete improved template matching, as shown in detail in Section 2.2.3, on the highest-level image of the image pyramid, obtain the score g, angle θ, and position coordinates.
Step 4: Set the lowest score value $g_{\min}$ to reduce the search time. The results of g and $g_{\min}$ are compared and determined. If $g \geq g_{\min}$, then it is an accurate target and searches the object again. Otherwise, it is not an accurate target and terminates the matching process.
Step 5: Place the matching results on the lower-level image matching. If the results fall on the lowest level, then skip to Step 7; otherwise, move to the next step.
Step 6: Track the next lower level and search the small area from the higher level matching results with improved template matching. Step 5 is then repeated.
Step 7: Analyze the matching results at the lowest level by polynomial fitting, and output the accurate result.

2.2.2 Hough transform and rough angle calculation

Hough transform can connect discrete edges into a line and can easily detect the lines and obtain the rough angle of the image because of the evident linear characteristics of the semiconductor chips. Hough transform method is used to process the contour of the binary images. The rough angles of the lines are calculated and recorded, and the statistical ranges are from 1° to 180°. By interval step of 1°, divide the data into several

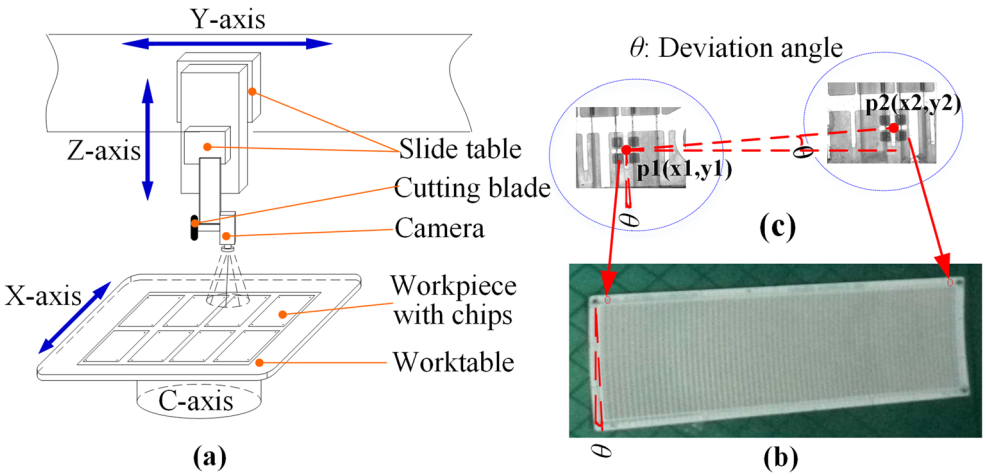

Fig. 1 **a** VPS for dicing **b** semiconductor chips by **c** matching special marks

sets and calculate the average of most members of the set. The different values between the rough angles are calculated by this method, and the actual angle is less than 1° through experimental verification.

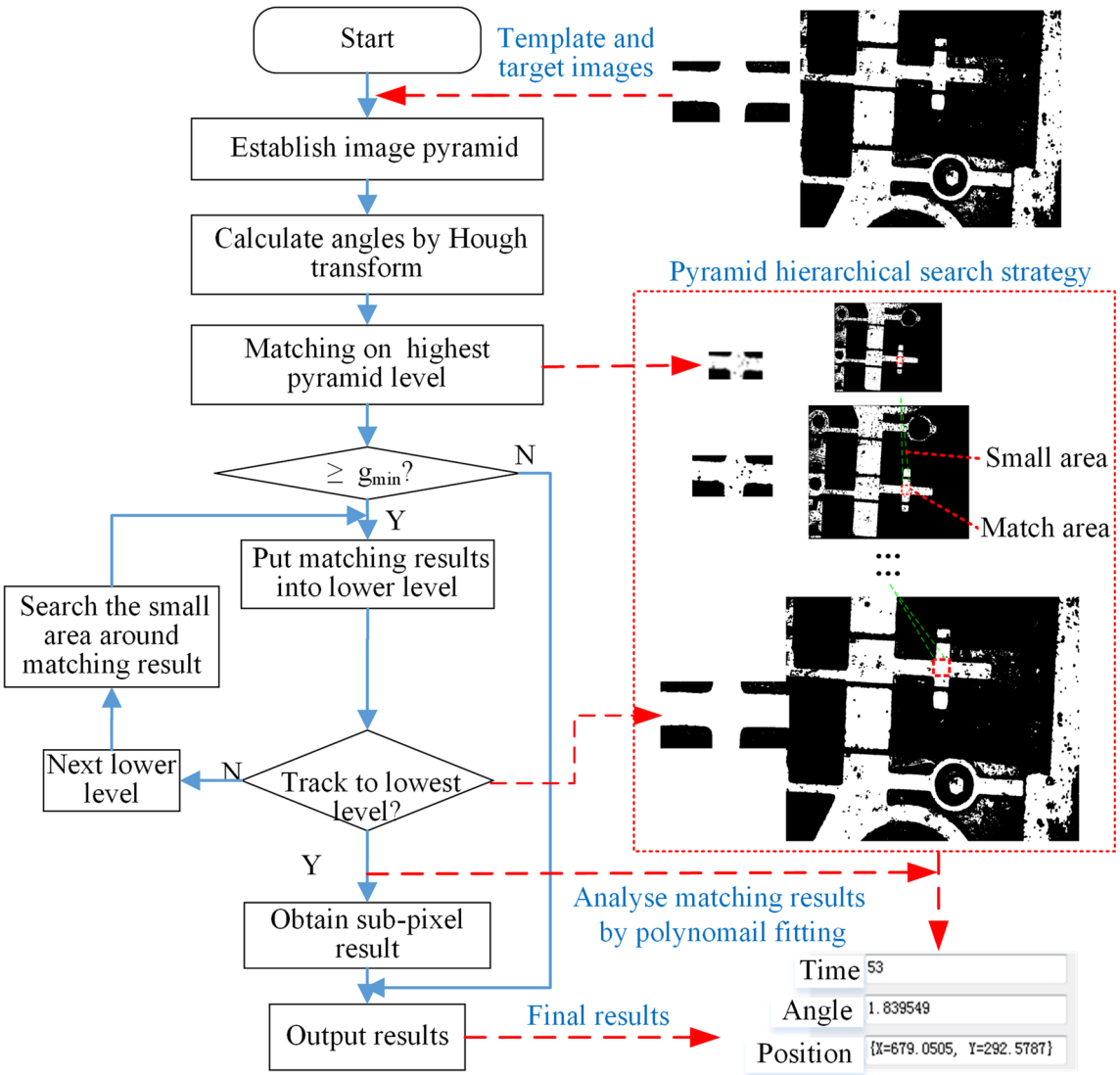

Fig. 2 Flow diagram of improved template matching algorithm

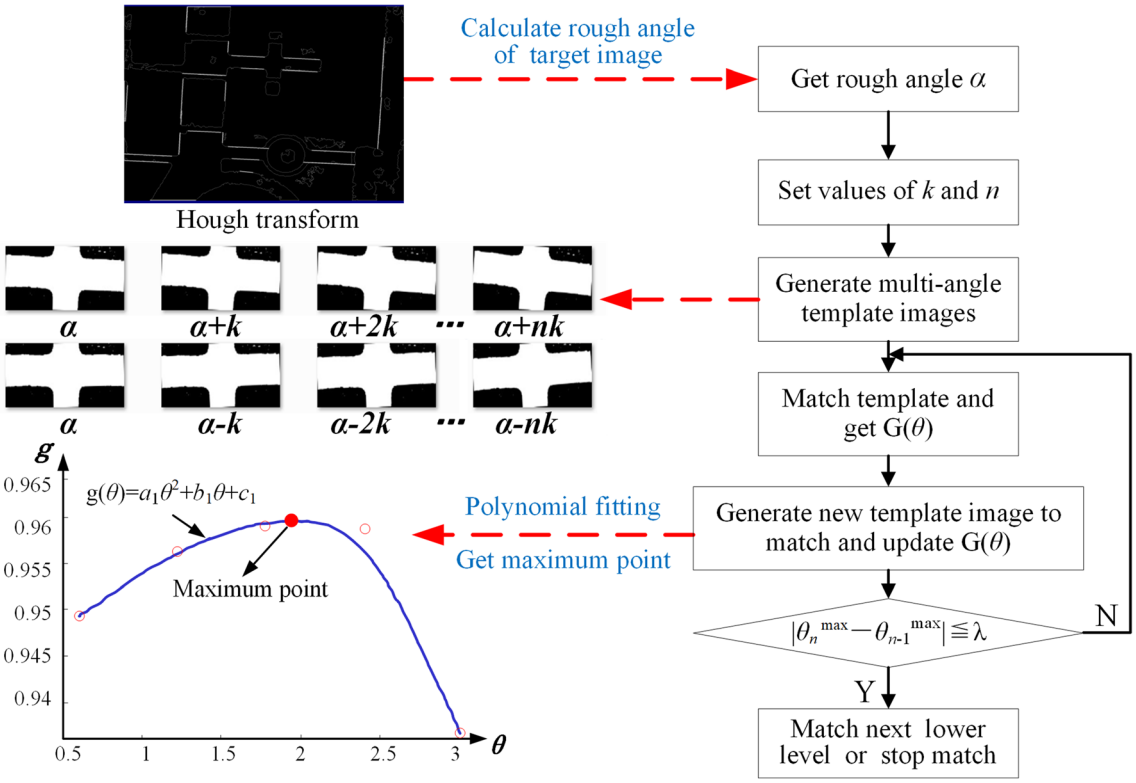

Fig. 3 Flow diagram of multi-template matching

2.2.3 Improved template matching

Conventional template matching can search the most similar portions of the larger image with a known template image. Although the method has low complexity and high stability, the computation speed cannot satisfy the real-time requirement of the VPS in dicing saw. The present work proposes an improved template matching algorithm based on the normalized cross-correlation (NCC) algorithm that belongs to a free distribution library (Opencv), and it is a classic template matching algorithm [20] to satisfy the production requirement, which includes rotation invariance, multi-target, and algorithm precision.

Rotation invariance A rapid and accurate method was proposed to obtain more precise angles and positions because the rough angle obtained by Hough transform cannot satisfy the actual requirements. Multi-angle template images were obtained from the searching process, and an iterative method was used to accelerate the search for the best angle. If the rough angle α is obtained by Hough transform, the range of the actual angle can be inferred from $\alpha-1.0$ to $\alpha+1.0$. First, the $2n+1$ template images are generated by taking α as the center in a step k, and each template image is matched with the target image by the NCC algorithm. A scoring array G(θ) is obtained as shown in Eq. (1), as follows:

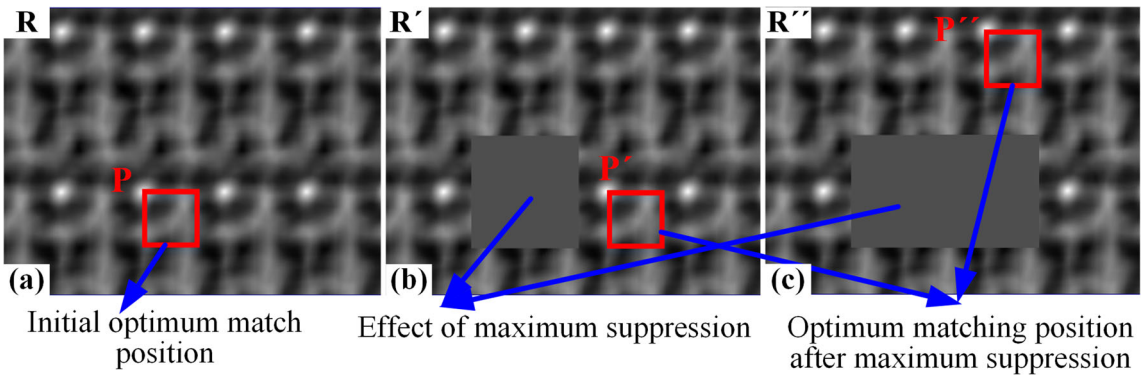

Fig. 4 Schematic diagram of maximum suppression

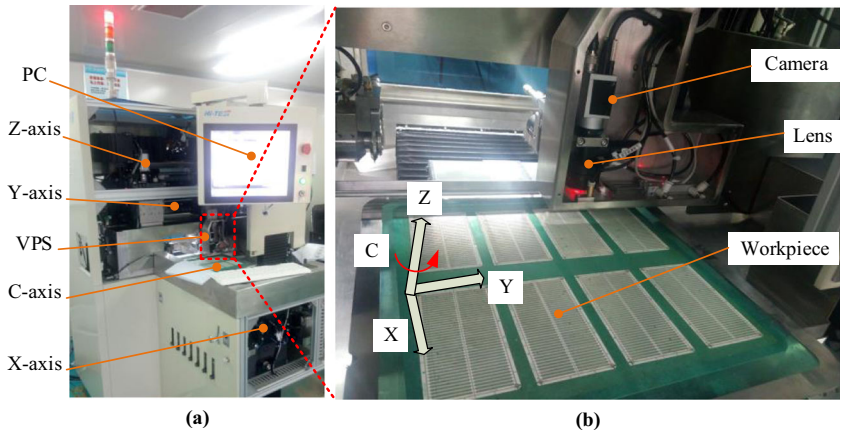

Fig. 5 **a** Experimental equipment with **b** VPS for dicing semiconductor chips

$$\begin{cases} G(\theta) = f_{NCC}(\theta) \\ \theta = \alpha \pm nk \end{cases} \quad (1)$$

where $f_{\mathrm{NCC}}(\theta)$ is the local maxima of NCC algorithm, and θ is the angle of template image. If the accuracy value k is extremely small, then the time consumption of the temple matching will increase dramatically. Therefore, the iterative method was used to accelerate the process of approaching the actual angle. G(θ) is updated after each iteration. The flow chart is shown in Fig. 3, and the specific steps are as follows:

Step 1: The rough angle α is obtained from Hough transform, and the values of k, n, and λ are set, and λ is the accuracy requirement of angle.

Step 2: The multi-angle template images are generated based on α, k, and n.

Step 3: The image from the multi-template images is matched to obtain G(θ), the maximum value of f NCC(θ) is f 0 NCC, and the corresponding angle θ0 max is obtained. Then, G(θ) is converted into a curve defined as $g(\theta) = a_1\theta^2 + b_1\theta + c_1$ by polynomial fitting. The coefficients a_1, b_1, and c_1 are solved by the least square method, and the angle $\theta^1_{\max}$ is obtained when the value of $g(\theta)$ is maximum.

Step 4: A new template image whose angle is θ1 max is generated and matched with the target image. Then, (θ1 max, f 1 NCC) is obtained and inserted into G(θ) in the order of θ. So far, G(θ), f NCC, and θ max is updated and one iteration is completed.

Step 5: Steps 3 and 4 are repeated a few times until the condition $|\theta t\ \max\text{-}\theta t\text{-}1\ \max| \leqq \lambda$ is satisfied, where λ is the accuracy of angle, and t is the iteration number.

Step 6: Let k be half of its original value, and n be 2. Track the next level or stop match.

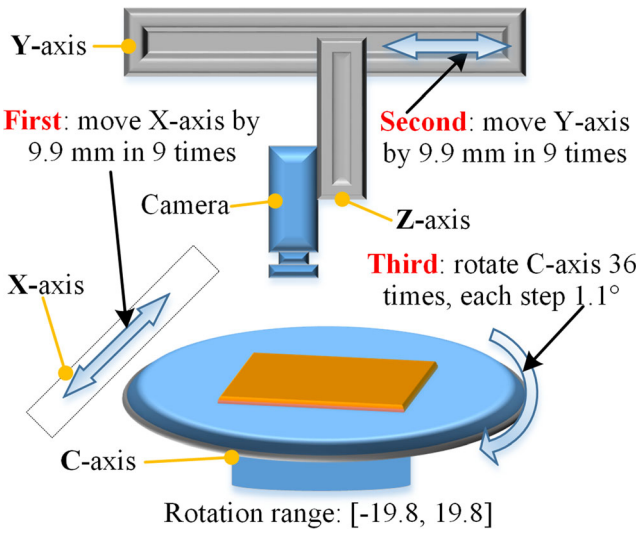

Fig. 6 Verification of position precision in three different cases

However, the number of iterations directly affects the consuming time of algorithm, and the accuracy of angle λ determines the number of iterations. So the λ is an important parameter. If the template image size (203 × 325) and target image size (1623 × 1236) remain constant, when the λ is set to 0.1, 0.5, and 0.05, the average time-consuming are 45.2, 30.5, and 65.1, respectively.

Multi-target matching The principle of NCC algorithm can be summarized as moving the template image over all pixels of target images and computing the cross-correlation at each pixels, then storing to the result matrix **R** and searching the extreme value as matching result. The extremum search and suppression of result matrix **R** from NCC algorithm were carried out in the searching process of multiple targets. The matrix **R** is shown in Fig. 4a, and the maximum $g_{\max}$ of **R** and position P are searched. After comparing $g_{\max}$ with $g_{\min}$ defined in Section 2.2.1, the maximum and P are stored in **R**. The pixel value in the rectangular area, where P is the center,

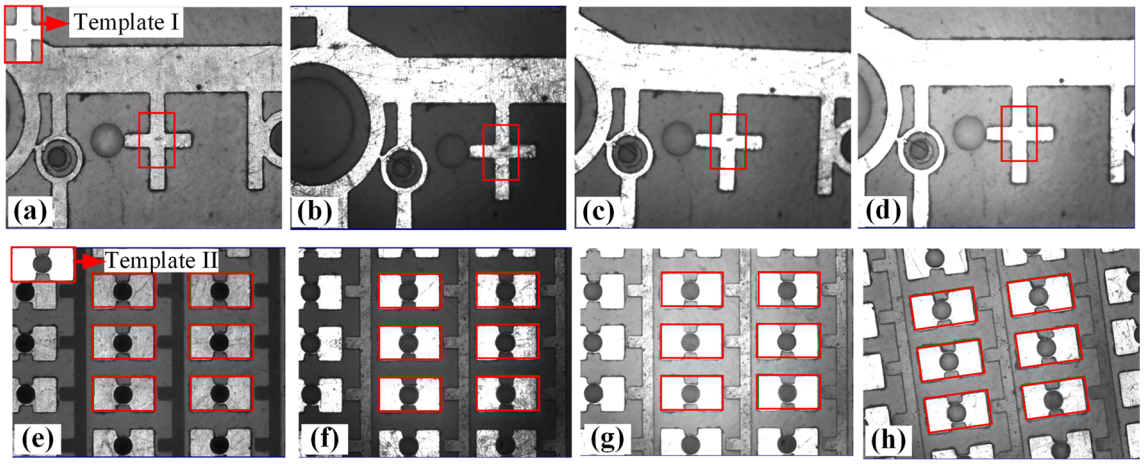

Fig. 7 Stability of the matching algorithm for the single target and the multiple targets under weak light (**a**, **e**); uneven illumination (**b**, **f**); strong light (**c**, **g**); and rotation conditions (**d**, **h**)

is set to a smaller value. Repeat the searching after new result matrices is obtained; all targets that are larger than $g_{\min}$ can be matched. The new result matrices $\mathbf{R}'$ and $\mathbf{R}''$ are obtained (Fig. 4b, c).

Improving position precision Though the position accuracy obtained by this matching method is pixel-level, it still cannot satisfy the quality requirements for dicing semiconductor ships. The matching precision should be enhanced by improving the algorithm to avoid increasing of hardware costs. The score values from the 3 × 3 neighborhood of the optimum matching in **R** can be analyzed by polynomial fitting, which is consistent with the angle fitting method. The fitting type is in binary quadratic form, and the equation can be expressed as follows:

$$g(x,y) = ax^2 + bx + cy^2 + dy + exy + f \tag{2}$$

where (x, y) are the pixel coordinates in the image. For the sample point $G(x_i, y_j)$ in the neighborhood, the error sum of squares can be calculated by as follows:

$$E(a,b,c,d,e,f) = \sum_{i=1}^{9} (g(x_i,y_i) - G(x_i,y_i))^2 \tag{3}$$

Table 1 Matching rates under different conditions

Different environment	Matching results	
	Single target	Multiple targets
Weak light	50/50	49/50
Strong light	49/50	49/50
Uneven illumination	50/50	50/50
Rotation	50/50	50/50
Matching ratio	99.5%	99%

After taking the partial derivatives of a, b, c, d, e, and f in Eq. (3) and making the results equal to zero, the parameter values can be obtained. The extreme point of Eq. (2) can be used as a new result by fitting the results obtained by the improved algorithm.

3 Experiments

3.1 Experimental setup

Matching experiment was carried out to verify the improved algorithm performance on an automatic dicing saw (Fig. 5). The VPS and the dicing blade were mounted on the Z-axis and can move in the vertical direction. The Z-axis table was installed on the Y-axis, which moves along the horizontal direction. The workpiece was placed on the workbench, which is fixed on the rotation table, and can rotate around the C-axis. The rotation table was installed on the X-axis table. The VPS mainly includes the CCD camera, lens, and light source. The camera model is Basler acA16-20gc with the frame rate of 20 fps, and the resolution is 1626 × 1236. The magnification of the lens is 1.5, and the working distance is 65 ± 1 mm. The depth of field of the lens is 0.4 mm. The light sources consist of a 100-lx ring light source and a 300-lx point light source.

3.2 Experimental conditions

The semiconductor material is LED, whose main components are the SiC, metal coating, and the epoxy resin film. The size of the material is 121 mm × 54 mm × 0.6 mm, and the dicing width is 340 μm. The dicing tool is a diamond blade bonded to the resin, the grit size is 700 mesh, and the thickness is 100 μm. The cooling water pressure and the gas supply pressure are 0.4 MPa. The spindle speed is 20,000 rpm, and the feed speed is 80 mm/s.

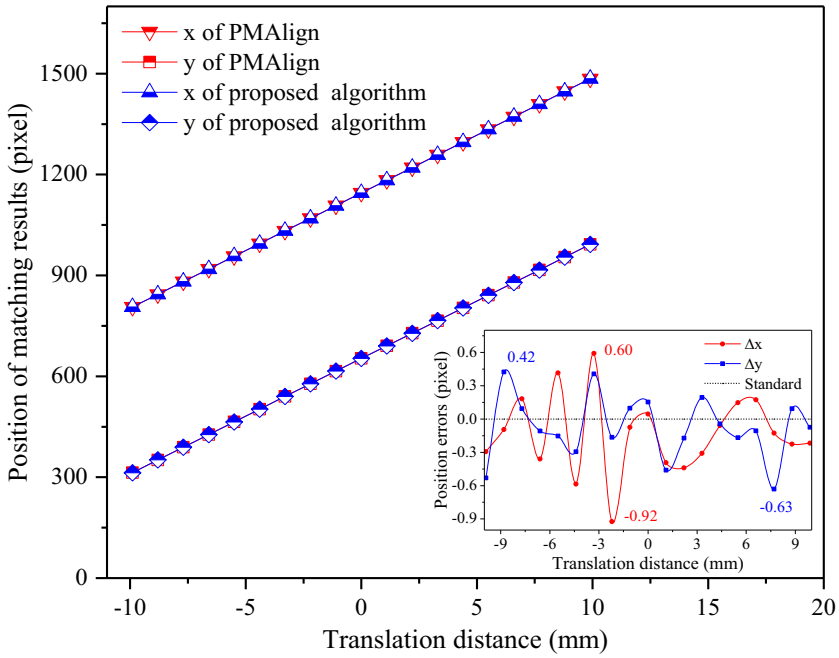

Fig. 8 Matching results of positioning precision

3.3 Vision positioning by improved template matching

3.3.1 Positioning stability

The uneven illumination, light intensity fluctuation, and chip rotation may occur when the semiconductor chips were diced on a dicing saw with VPS in Fig. 6. The positioning experiment was carried out to match four group pictures under weak light (approximately 150 lx), strong light (approximately 800 lx), uneven illumination, and rotation conditions to verify the stability of the improved template matching algorithm. Each group contains same size 50 pictures obtained under four conditions mentioned above.

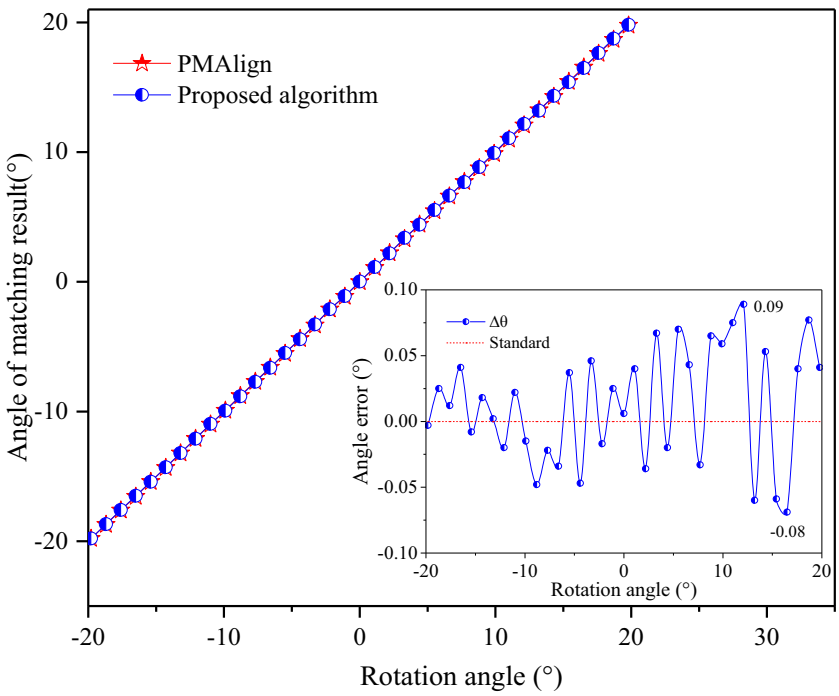

Fig. 9 Matching results of angle precision

Table 2 Time-consuming of two algorithms

Template size (pixel)	Time-consuming (ms)		Improve rate (%)
	Improved algorithm	NCC algorithm	
163 × 285	33.8	144.8	144.8
203 × 325	45.2	171.5	171.5
224 × 386	56.6	193.6	193.6
264 × 386	63.6	225.4	225.4

3.3.2 Positioning precision

The control variable method was used to obtain the position precisions at *x*-*y*-directions and angle precision. A special mark was selected as a template image, and then the target images were collected in three different situations. In the first case, the workpiece moved 9.9 mm nine times along the *x*-direction, and the image was matched during each time searching. The workpiece also moved 9.9 mm nine times along the *y*-direction, and the image was matched. In the third case, the workpiece rotated 1.1° in each step around C-axis, and the rotation time was 36 at the rotation range of [− 19.8, 19.8]. The three sets of images were matched with the improved algorithm and the algorithm (PMAlign) of VisionPro®8.2 SR1 developed by Cognex corporation under the same conditions. VisionPro® is a very commercial vision library for leading PC-based vision software. The tool library performs a wide range of functions from geometric object location and inspection to identification and measurement. However, the VisionPro® tool is like a black box for us, and we cannot find the real underlying matching algorithm. The results were compared based on the standard of PMAlign results. The comparison error is expressed as Δx in the *x*-direction. The error Δy is expressed in the *y*-direction, and $\Delta\theta$ is the error of the rotation angle.

3.3.3 Positioning speed

The positioning speed using the improved algorithm was compared with that using the NCC algorithm. The specifications of the hardware and software platforms were as follows: Window 7, dual-core Intel(R), Pentium(R), 3.3GHz CPU, and 2.0G of memory. Four groups (50 images per group) of template images with different sizes were used. The sizes of the template images were 163 × 285, 203 × 325, 224 × 386, and 264 × 386, and the size of the target image was 1623 × 1236.

3.3.4 Dicing semiconductor chips

When the accuracy and speed of the improved algorithm had been verified to satisfy the requirements of high-precision dicing semiconductor chips, the algorithm of vision positioning was used to position the eight workpieces with many semiconductor chips. The dicing experiment was conducted, and the dicing results were measured by the Olympus STM6 and the digital microscope VHX-5000.

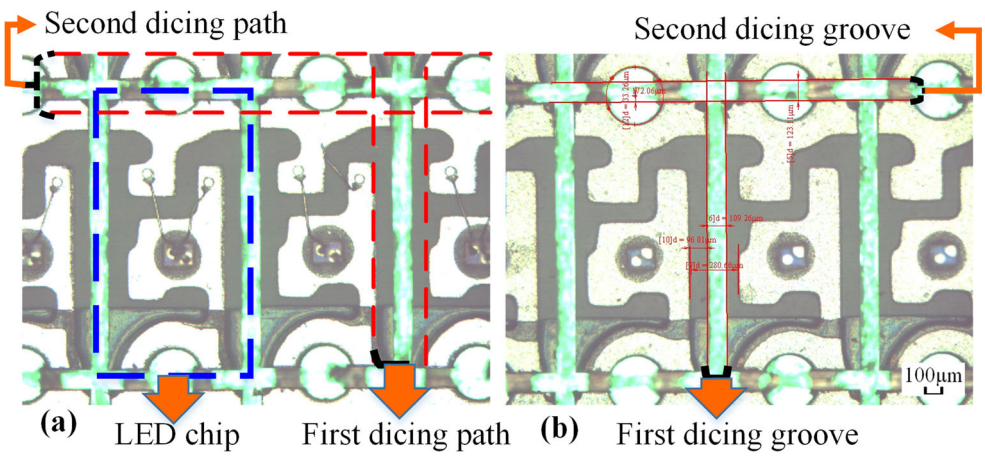

Fig.10 **a** Diced semiconductor chips and **b** measured results

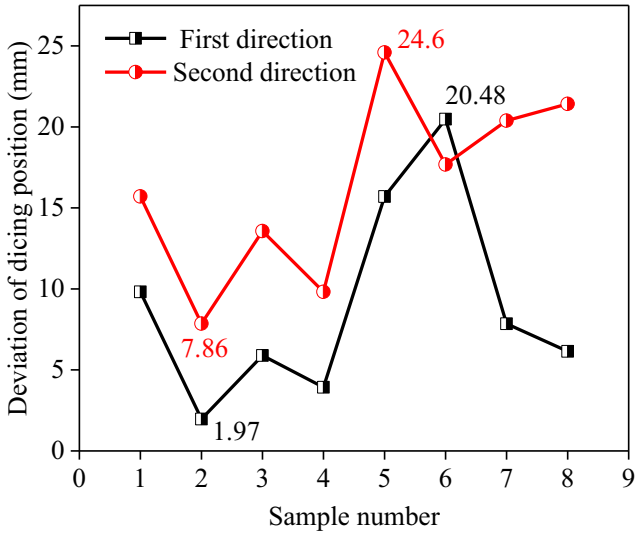

Fig. 11 Dicing position deviation in first and second directions

4 Results and discussions

4.1 Positioning stability

Figure 7 shows the typical matching results under four different conditions. Table 1 shows the successful rates of single target and multiple targets. The success rate of a single target is higher than that of the multiple targets because the matching score is lower when the light is strong or weak, and matching some targets is difficult when the scores under the multiple target conditions are lower than g_{min}. The success rate of strong light is lower than the other light conditions because distinguishing the background and target images is more difficult under the strong light condition, as shown in Fig. 7g. However, the algorithm can almost identify all targets even under some poor light environment, and the matching rate is up to 99.25%.

4.2 Positioning precision

Figure 8 shows the comparative position errors between the improved and PMAlign algorithms. The maximum position error in *x*-direction is 0.92 pixels, and the standard deviation is 0.34. The maximum error in *y*-direction is 0.63 pixels, and the standard deviation is 0.28. The small position error and error variance indicate that the algorithm has the characteristic of high repeatability. The algorithm precision in *y*-direction is higher than that in *x*-direction because of the slight deviation of matching angle which affects the position error. By rotating the template in the image coordinate system, it can find that the position error in *x*-direction is positively correlated with the height of the template image, and the position error in *y*-direction is also positively related to the width. The template size is 163 × 366 pixels, and the height is 2.24 times as the width, thereby resulting in a larger error in *x*-direction than in *y*-direction.

Figure 9 shows the comparative angle error between the improved and PMAlign algorithms. The maximum angle error is less than 0.09°, and the standard deviation is 0.004. The angle accuracy is extremely high, and the position error in *y*-direction is smaller than that in *x*-direction because of the improved multi-template matching algorithm. Therefore, the accuracy of the proposed algorithm can satisfy the requirements of the actual processing.

4.3 Positioning speed

Table 2 shows that the number of template image's pixels is 100 thousand, the time consumption of the proposed algorithm is still less than 80 ms and the total time consumption is approximately 1/4 of the conventional template matching algorithm. Therefore, the real-time requirement can be satisfied. Moreover, when the template image size is large, the improved rate is high because the NCC algorithm consumes

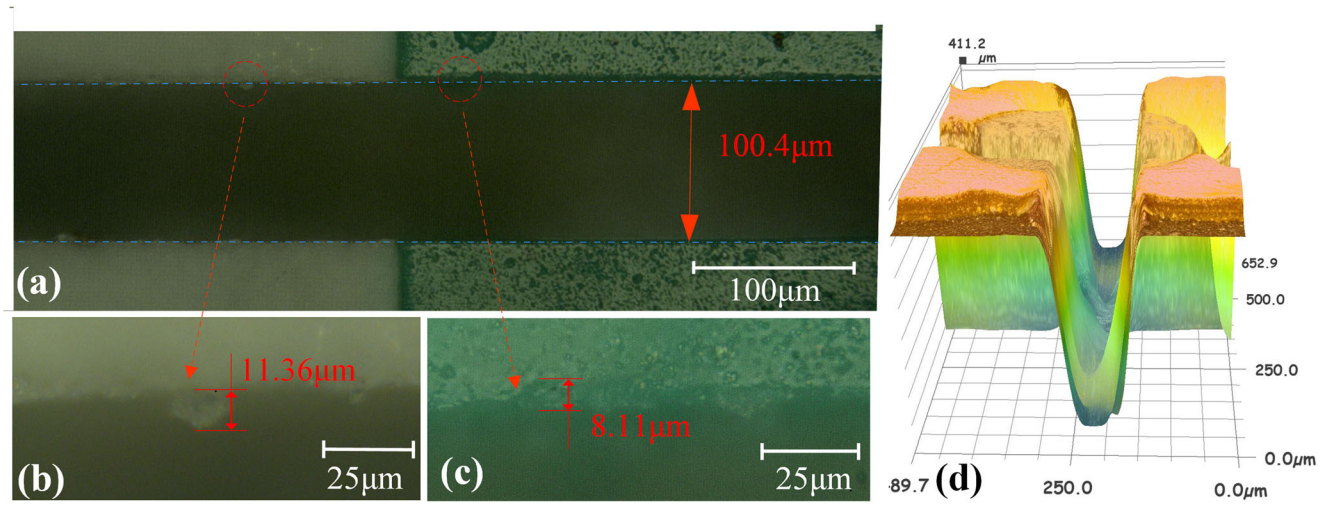

Fig.12 **a** The width of the dicing groove with a burr (**b**) and a breakage (**c**) and 3D sectional view (**d**)

much time and the pyramid search strategy accelerates rapidly when the template image size is large.

4.4 Dicing precision

The special marks of the semiconductor chips are searched and recognized by VPS with the improved algorithm. After completing the dicing process, the Olympus-Stm6 is used to measure the cutting grooves of the semiconductor chips. The magnification is 5, and the size of the actual image is 3.45 μm. As shown in Fig. 10, important results on the diced workpiece include the dicing path width, the dicing groove width, and the deviations between the dicing path and the edge of the dicing groove in the first and second directions. The deviation at the first direction is related to the matching position error in *y*-direction, and the deviation at the second direction is related to the matching position error in *x*-direction.

The maximum permissible deviation between the cutting groove and dicing path is ± 30 μm when dicing semiconductor chips. Figure 11 shows the measurement results. The maximum deviation of the dicing position at the first direction is 15.7 μm, the average is 8.97 μm, and the variance is 5.82. The maximum deviation is 24.60 μm, the average is 16.38 μm, and the variance is 5.41 at the second direction. The deviations are less than 30 μm, thereby indicating that the matching positioning accuracy is relatively stable. The deviation at the first direction (Y-axis) is smaller than that at the second direction (X-axis) because it is affected by the algorithm's precision at different directions. Therefore, the precision in *y*-direction is higher than in *x*-direction. Figure 12 shows the two-dimensional and three-dimensional images of the dicing groove measured by VHX-5000. The dicing groove width is 100.4 μm, the maximum breakage is 8.11 μm, and the maximum burr is 11.36 μm, respectively, which shows that the dicing quality is also excellent.

5 Conclusions

An improved matching algorithm for vision positioning is proposed to dice semiconductor chips by using the gray scale and line characteristics. The experimental results show that the improved algorithm can match almost all targets even under the conditions of weak light, strong light, uneven illumination, and rotation angle. The success rate is 99.25% when matching the single and multiple targets. The position and angle errors are less than 1 pixel and 0.08°, respectively, comparing with the algorithm from VisionPro® 8.2 SR1. The time consumption is only 1/4 of the NCC algorithm. The dicing experiment is carried out on a dicing saw with VPS. The dicing deviation is less than 25 μm, and the breakage is only 2.66 μm, thereby satisfying the dicing requirement. The dicing results confirm that the improved algorithm could be used for high-precision and real-time dicing of semiconductor chips.

Funding information This work is financially supported by the Science and Technology Project of Hunan Province (No. 2017WK2031).

References

1. Araujo LAO, FoschiniR CR, Jasinevícius G, Fortulan CA (2016) Precision dicing of hard materials with abrasive blade. Int J Adv Manuf Technol 86:2885–2894
2. Wang Z, Gong S, Li D, Lu H (2017) Error analysis and improved calibration algorithm for LED chip localization system based on visual feedback. Int J Adv Manuf Technol 92:3197–3206
3. Korman S, Reichman D, Tsur G, Avidan S (2017) Fast-match: fast affine template matching. Int J Comput Vis 121:111–125
4. Cui DY, Gao WT, Xia KW (2017) Image denoising of strip steel surface defects based on K-SVD algorithm. Surface Technology 46:249–254. https://doi.org/10.16490/j.cnki.issn.1001-3660.2017.05.040
5. Peng X, Xu J (2016) Hash-based line-by-line template matching for lossless screen image coding. IEEE T Image Process 25:5601–5609
6. Bao G, Cai S, Qi L, Xun Y, Zhang LB, Yang QH (2016) Multi-template matching algorithm for cucumber recognition in natural environment. Comput Electron Agr 127:754–762
7. Kim HY (2010) Rotation-discriminating template matching based on Fourier coefficients of radial projections with robustness to scaling and partial occlusion. Pattern Recogn 43:859–872
8. Feng Y, Ren J, Jiang J, Halvey M, Jose JM (2012) Effective venue image retrieval using robust feature extraction and model constrained matching for mobile robot localization. Mach Vision Appl 23:1011–1027
9. Mattoccia S, Tombari F, Di Stefano L (2011) Efficient template matching for multi-channel images. Pattern Recogn Lett 32:694–700
10. Yu X, Fei X (2017) Target image matching algorithm based on pyramid model and higher moments. J Comput Sci 21:189–194
11. Liang J, Liao Z, Yang S, Wang Y (2012) Image matching based on orientation magnitude histograms and global consistency. Pattern Recogn 45:3825–3833
12. Matsuda Y, Miura N, Nagasaka A, Kiyomizu H, Miyatake T (2016) Finger-vein authentication based on deformation-tolerant feature-point matching. Mach Vision Appl 27:237–250
13. Cui X, Kim H, Park E, Choi H (2013) Robust and accurate pattern matching in fuzzy space for fiducial mark alignment. Mach Vision Appl 24:447–459
14. Yan W, Tian Z, Duan X, Pan L (2013) Feature matching based on unsupervised manifold alignment. Mach Vision Appl 24:983–994
15. Yasseen Z, Verroust-Blondet A, Nasri A (2016) Shape matching by part alignment using extended chordal axis transform. Pattern Recogn 57:115–135
16. Yang C, Tiebe O, Shirahama K, Grzegorzekl M (2016) Object matching with hierarchical skeletons. Pattern Recogn 55:183–197
17. Zhong FQ, He SP, Li B (2017) Blob analyzation-based template matching algorithm for LED chip localization. Int J Adv Manuf Technol 93:55–63
18. Wang ZY, Gong SH, Li DL, Lu HQ (2017) Error analysis and improved calibration algorithm for LED chip localization system based on visual feedback. Int J Adv Manuf Technol 92:3197–3206
19. Kondo T (2014) Gradient orientation pattern matching with the Hamming distance. Pattern Recogn 47:3387–3404
20. Brown LG (1992) A survey of image registration techniques. ACM Comput Surv 24:325–376